Eur. Phys. J. E (2013) **36**: 140
DOI 10.1140/epje/i2013-13140-x

THE EUROPEAN PHYSICAL JOURNAL E

Regular Article

Ripple formation in unilamellar-supported lipid bilayer revealed by FRAPP

Frédéric Harb[1], Anne Simon[2,a], and Bernard Tinland[1,b]

[1] CNRS, UMR7325, Aix-Marseille Univ., CINaM, 13288, Marseille, France
[2] Institut de Chimie et Biochimie Moléculaires et Supramoléculaires, Université Lyon 1, University of Lyon, ICBMS, CNRS UMR 5246, Bât. Curien, 43 bd du 11 Nov. 1918, F-69 622 Villeurbanne cedex, France

Received 6 September 2013 and Received in final form 20 November 2013
Published online: 17 December 2013 –

Abstract. The mechanisms of formation and conditions of the existence of the ripple phase are fundamental thermodynamic questions with practical implications for medicine and pharmaceuticals. We reveal a new case of ripple formation occurring in unilamellar-supported bilayers in water, which results solely from the bilayer/support interaction, without using lipid mixtures or specific ions. This ripple phase is detected by FRAPP using diffusion coefficient measurements as a function of temperature: a diffusivity plateau is observed. It occurs in the same temperature range where ripple phase existence has been observed using other methods. When AFM experiments are performed in the appropriate temperature range the ripple phase is confirmed.

List of abbreviations

SLB: Supported Lipid Bilayer
SUV: Small Unilamellar Vesicle
LUV: Large Unilamellar Vesicle
MLV: Multi Lamellar Vesicle
FRAPP: Fluorescence Recovery After Pattern Photobleaching

1 Introduction

From a biological point of view, it has been suggested that the membrane state and/or its local curvature could be involved in bioactivity. Consequently, species (alcohol, protein, etc.) could be added to modulate this bioactivity [1, 2], offering great potential for medical and pharmaceutical applications.

Lipid bilayers have proved valuable as synthetic systems to study cell membranes. The different phase states and transition from one to another have been explored in numerous studies [3–6]. At low temperature (T), lipids are in the gel phase state (L_β), with chains tilted with respect to the membrane plane. When the temperature increases, the tilt angle changes: this transition is called the pretransition. At higher temperatures, lipids present a change in the hydrocarbon chain conformation: this transition is called the main transition. After this transition, all lipids are in the fluid state (phase L_α). Depending on experimental conditions, there may be an intermediate phase P_β, of a two-dimensional order, containing lipids either in gel or fluid phase, called the ripple phase [5,7,8].

The formation, amplitude and periodicity of ripple structures have been studied using freeze-fracture electron microscopy, AFM, DSC, X-Ray, neutron scattering, SANS and SAXS [5,9–16]. The ripple phase has been established as occurring in large unilamellar vesicles (LUVs), in multilamellar vesicles (MLVs) and on top of supported double bilayers [17–19], this last case being, in fact, a particular type of multi-bilayer. The common characteristic of these systems is that they allow large geometric fluctuations of the membranes. In unilamellar-supported bilayers (or single supported bilayers), it can be expected that the ripple phase does not exist because the proximity of the support prevents geometric membrane fluctuations. However, it has been reported to appear in unilamellar bilayers, although only in two cases: i) in bilayers composed of a mixture of two different lipids [20]; ii) when specific ions like Tris are present [21]. It has also been shown that the ripple phase sometimes cannot appear *i.e.*, when there are lateral constraints [13].

Thus, the conditions necessary to produce the ripple phase remain both elusive and challenging. A fundamental thermodynamic question is that of its formation and evolution mechanisms. Differing models have been

[a] *Current address*: Laboratoire Chimie et Biologie des Membranes et des Nanoobjets, Université Bordeaux, CBMN, UMR 5248, Allée Geoffroy St Hilaire, F-33600 Pessac, France.
[b] e-mail: tinland@cinam.univ-mrs.fr

proposed to describe ripple phase structures [4,8,21–24]. Some suppose a variable thickness and possible leaflet decoupling [25,26]. Others propose a constant thickness [20, 23,27]. Simulations have shown that both structures are possible [20,28]. It was Heimburg [29] who proposed the ripple phase as an intermediate state linking the pretransition and the transition, having a temperature range which depends on the lateral object compressibility. He described the resulting conformation of a given bilayer as the result of the constraints exerted by two rigid walls (formed by the other bilayers), as the resultant of the value of the free energy (ΔG), as a function of system conditions [25].

Tamm *et al.*, observing a plateau on its diffusion coefficient $D = f(T)$ curve [30], were the first to mention the possibility that it was of a ripple phase occurring in a DPPC/SiO_2/H_2O unilamellar-supported bilayer. Previous works had revealed the existence of a plateau on $D = f(T)$ curves in the temperature range where ripple phase formation was known to occur [31,32], but this avenue had not been explored.

In this work we address the question of whether ripple formation can occur solely through the interaction of a single bilayer with its support (only one bilayer, one lipid, no specific ions), using Fluorescence Recovery After Patterned Photobleaching (FRAPP) curves as a detection tool.

2 Materials and methods

2.1 Sample preparation

All lipids were purchased from Avanti Polar Lipids and used without further purification. SLBs were prepared using either 1,2-dimyristoyl-sn-glycero-3-phosphocholine (DMPC) or 1,2-dipalmitoyl-sn-glycero-3-phosphocholine (DPPC). The fluorescence recovery experiments required the incorporation of a small fraction of fluorescently labelled phospholipid in the samples (0.1%). We used fatty acid labelled lipids with NBD (nitrobenzoxadiazole): 14:0-6:0 NBD PC for DMPC and 16:0-12:0 NBD PC for DPPC. The placing of fluorescent markers is subject to some debate. If placed on the PC head, therefore in the aqueous phase, they could alter the "natural" interaction of the proximal leaflet of the bilayer with the support. Thus, we chose to use a lipid with the marker on an arm, therefore in the hydrophobic phase, such that the resulting length is the same as the length of the lipid chain without markers. Since the proportion of lipids bearing a marker is very low (0.01%), the diffusion coefficient can be expected to be negligibly affected. Additionally, since all systems (lipid bilayers on solid supports) have the same bilayer composition, they can be compared for the purposes of our study.

Two kinds of support were used: either freshly cleaved mica (Muscovite, scratchless grade, JMG Metafix, France) or microscope glass slides (Marienfeld, pre-cleaned, cut edges, France). Glass slides were cleaned for 10 minutes in fresh alcoholic NaOH and then extensively rinsed and sonicated in ultra-pure water 3 times. These substrates were chosen, not on a technological or biophysical basis, but because the behaviour of lipids on glass and mica is well documented, thus enabling us to compare data with values from the literature (*i.e.* value of D in the fluid phase, difference in zeta potentials, sign of the surface). This makes it possible to verify data quality and absence of artefacts, as well as shedding light on the thermodynamics behind these systems

2.2 Langmuir-Blodgett and Langmuir-Schaefer depositions

The Langmuir-Blodgett (LB) transfer technique was used to prepare bilayers supported on planar hydrophilic substrates [30]. Lipid molecules solubilised in chloroform ($\cong$ 1 mg/ml) were deposited on the water subphase (18 MΩ cm, MilliQ, 15 °C) of the Langmuir trough (KSV Minitrough 361 mm × 74 mm, Finland), equilibrated for 10 minutes to allow complete solvent evaporation and then compressed to the desired pressure (30 mN/m for DMPC and 40 mN/m for DPPC). For double Langmuir-Blodgett depositions on mica, the substrate (25 mm × 25 mm) was dipped up and down at a speed of 5 mm/min. When it was not possible to deposit the second monolayer without quantitatively peeling off the first monolayer, namely with the glass used here, an alternative method consisted in using the out-of-equilibrium Langmuir-Schaefer (LS) technique: after the first monolayer LB deposition, the "hydrophobic" substrate in air was rotated to the horizontal position, and lowered through the interfacial monolayer (for details, see [33]) in order to close the bilayer with the second monolayer. The fact that double LB deposition is possible only on mica indicates a higher lipid/support interaction than with our glass (LB+ LS required). The transfer ratio was defined as the decrease in water-air monolayer area during deposition divided by the area of the substrate brought through the monolayer. It strongly influences the quality of samples, as shown by structural studies based on AFM [34], or neutrons and X-ray reflectivity measurements [33]. Here, transfer ratios were close to 1.12 for all monolayers, indicating *a priori* high quality bilayers. Bilayers were kept constantly under water after fabrication.

2.3 Preparation of SLB by vesicle fusion

Small unilamellar vesicles (1 mg/ml) containing DMPC were produced by extrusion. Lipids were dissolved in 1 mL of chloroform and subsequently dried in an argon flow. After 30 min, the lipids were re-suspended in Hepes buffer (150 mM NaCl, 10 mM HEPES, pH 7.4) and vortexed for 5 min. The suspension was extruded 20 times through a 100 nm polycarbonate membrane (Avanti Polar Lipids, U.S.A.) and then 20 times through a 50 nm polycarbonate membrane using an Avanti Polar Lipids extruder. The final vesicle suspension was stored at 4 °C. SLBs were formed by deposition of SUVs at a final concentration of 0.5 mg/mL diluted in the following buffer: 10 mM HEPES, pH 7.4, 150 mM NaCl, and 2 mM $CaCl_2$ for 60 min onto

a cleaved mica surface and at room temperature. Excess vesicles and ions were removed by replacing the solution covering the mica surface several times with ultrapure water. Then, the samples were incubated for 12 hours at 4 °C.

2.4 FRAPP measurements

We used Fluorescence Recovery After Pattern Photobleaching (FRAPP) [35] to investigate the diffusion of lipids in the SLB. Briefly, the light beam of an etalon-stabilized monomode Ar laser (1 W at 488 nm) was split and the two equivalent beams crossed on the sample, providing an interference fringe pattern. The fringe spacing $i = 2\pi/q$ (set by the crossing angle θ, $q = 4\pi/\lambda \sin(\theta/2)$ is the wave vector) ranged from 1 to 80 μm and defined the diffusion distance. A bleach pulse set to 1 s with 0.5 W laser intensity wrote a fringe pattern into the sample, which, due to diffusion, disappeared with time. After the bleach pulse, the beam intensity is reduced to a few milliwatts: under these circumstances, we observed no further bleaching of the labelled lipids. We had a long time previously carried out tests to assess any dependence on laser intensity (data not published). Increased bleaching (adjusting bleach time or laser intensity) induces more bleached lipids, which impacts the amplitude of the contrast. However the relaxation time (thus the diffusion coefficient) remains constant whatever the bleaching conditions. One advantage of our set-up is that the bleaching pattern is exactly the same as the reading pattern. The set-up changes from one pattern to the other only by virtue of a Pockels cell. In view of the difference between bleaching intensity ($\cong$ 0.5 W) and reading intensity ($\cong$ mW), the relevant optical difference is between bleached and unbleached regions, and not within the fringes themselves. In regions illuminated by the bleaching laser intensity, the quantity of light is sufficient to bleach all the fluorophores, despite the sinusoidal shape of the pattern or the Gaussian shape of the laser beam.

If there is only one diffusive species, the recovery is of single-exponential nature. Considering Fick's law and the conservation equation, we get

$$\delta c(r,t)/\delta t = D\Delta c(r,t),$$

where $c(r,t)$ is the local concentration of the fluorescent molecules and D the diffusion coefficient.

Supposing an infinite medium, performing its Fourier transform, the equation becomes

$$\delta c(q,t)/\delta t = -q^2 D c(q,t),$$

q being the wave vector.

The solution to the equation is

$$c(q,t) = c(q,0)\exp(-Dq^2 t),$$

where $c(q,0)$ is the fluorescent molecule concentration in the Fourier space immediately after the bleaching.

The characteristic recovery time by means of Brownian diffusion is thus

$$\tau = 1/Dq^2.$$

Curves of fluorescence recovery (more precisely, curves of disappearance of contrast in this set-up) are fitted with

$$C(t) = C_\infty + (C_0 - C_\infty)\exp(-t/\tau),$$

C_0 and C_∞ being the contrasts just after and a very long time after the laser bleaching. Since D results simply from the above (Fick's law and mass conservation), there was no specific model related to the dimensions of the diffusion (such as, for instance, 1-dimensional in the ripple phase and 2-dimensional in other phases). Error bars in figures refer to standard deviation obtained from diffusion measurements at different temperatures, each consisting of 5–7 measurements.

The following two special features of the set-up are worthy of note: i) The use of the same periodic sinusoidal pattern for bleaching and reading allows a single mode of the diffusion equation to be probed. The analysis is more precise and thus it is easier to detect small variations in the diffusion coefficient, or to discriminate between different populations. ii) The experimental set-up also makes it possible to easily vary the interfringe value and to directly check the validity of the diffusion law in the reciprocal space.

To test whether the diffusion was Brownian or not, we carried out measurements at differing fringe widths (from 1 to 80 μm) at different temperatures: τ_q was always proportional to q^2. In the work reported here, considering the good transfer ratios, the fact that the relaxation time was always inversely proportional to q^2 in FRAPP experiments and the reproducibility of both quantities, we deduce that our bilayers have almost "infinite surface" and are without defect. This is confirmed by large-scale AFM images, which show no defects (data not shown).

2.5 Atomic Force Microscopy (AFM)

The DMPC SLBs were observed in the temperature range of the plateau $D = f(T)$ and at higher temperatures by *in situ* AFM. Images were acquired in milliQ water, in contact force mode and using a silicon nitride cantilevers with a 0.06 N/m nominal spring constant, at scanning rates of 2-3 Hz and a scan angle of 90°. All images shown were recorded at the lowest possible imaging force. They were flattened and analyzed using the standard 2D Fourier method.

3 Results and discussion

3.1 Diffusion of lipids of the top bilayer of a supported double bilayer

Figure 1 shows the changes in diffusion coefficient (D) as a function of temperature (T) for lipids of the second bilayer of a double DPPC bilayer (only the lipids of the second bilayer were labelled) obtained by Langmuir Blodgett deposition onto a mica support.

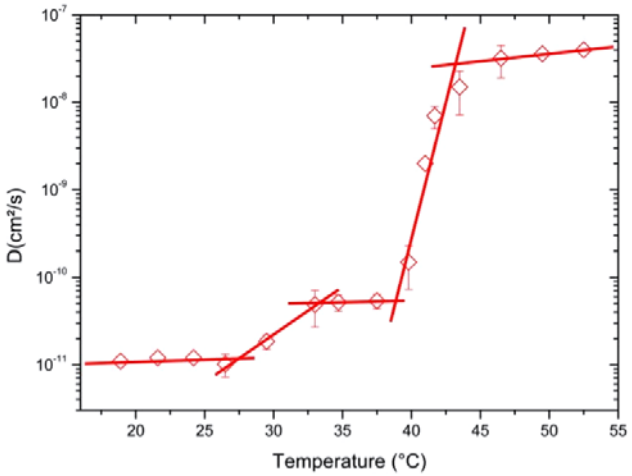

Fig. 1. Diffusion coefficient as a function of temperature of DPPC lipids of the second bilayer on mica. The lines represent the fit of the curve in different regimes.

The ripple phase is known to occur on double bilayers [18,19,21], and this constitutes the simplest and most well-controlled multi-bilayer system for lipid diffusion in ripple phase.

Figure 1 shows three regimes where the diffusion coefficient is almost constant. They correspond at low temperature (17 to 27 °C) to the gel phase (L_β) and at high temperature (higher than $\sim$ 42 °C) to the fluid phase (L_α). Between these two regimes, or between $\sim$ 27 °C and $\sim$ 42 °C, temperature increase results in a diffusion coefficient increase, except in a temperature gap from 33 to 39 °C. The appearance of a plateau in diffusion for the range of temperatures between pretransition and transition suggests an intermediate phase. The temperature range of the plateau is in good agreement with the temperature range observed by AFM and DSC experiments [36] on vesicles where a ripple phase was reported to exist. If we assume that this double layer system presents a ripple phase [18,19,21], the plateau in diffusion can be taken as a signature of the ripple phase.

3.2 Diffusion of lipids of a unilamellar-supported bilayer

Figure 2 shows curve $D = f(T)$ over a wide temperature range for two different lipids (DMPC and DPPC) in unilamellar bilayers supported on two different supports (mica and glass).

Figures 2a and b show the diffusion coefficients *vs.* temperature on mica. FRAPP signals are biexponentials corresponding to two values for diffusion coefficients and to the decoupling of distal and proximal leaflets due to a stronger interaction with mica [37].

The DPPC results on a unilamellar bilayer are similar to those observed in the previous situation on a double bilayer of DPPC supported on mica with respect to the different regimes (fig. 1). The diffusion coefficient of this bilayer, close to the support, is slower than for the second bilayer, far from the support, due to the higher interaction [38].

For both lipids DPPC and DMPC in unilamellar-supported bilayers, the observed diffusion coefficients *vs.* temperature are qualitatively the same. Gel phase and fluid phase appear at low and high temperatures, respectively, due to their different hydrocarbon lengths. There is also a temperature gap and a plateau in diffusion (19 to 23.5 °C for DMPC and 31.3 to 37.5 °C for DPPC) of roughly 5-6 °C.

For the purposes of comparison, figs. 2c and d show the diffusion coefficient for unilamellar-supported bilayers of DMPC and DPPC on glass. On this support, all diffusion coefficients are faster than on mica. All FRAPP signals are monoexponentials indicating no leaflet decoupling [37]. As previously observed, D is almost constant at low temperatures, corresponding to the gel phase (L_β). From 13.5 °C to 20.3 °C for DMPC and from 27.9 °C to 36.3 °C for DPPC, D increases with T, corresponding to the pretransition. From 20.3 °C to 26.5 °C for DMPC and from 36.3 °C to 45.5 °C for DPPC, the slopes increase further, corresponding to the main transition. At higher temperatures, D is again almost constant: this regime corresponds to the fluid phase L_α. These behaviours correspond to gel phase region, pretransition, main transition and fluid phase region, whatever the lipids used. The change in temperature range over the full transition from one lipid to the other is again due to their different hydrocarbon lengths. The main difference from the case detailed in figs. 2a and b is that no plateau is observed between pretransition and transition.

Assuming that the plateau is a sign of ripple phase existence, this suggests that it may originate from lipid-substrate interactions [39]. As the plateau is detected only on mica, the results confirm a stronger interaction of lipids on mica than on glass.

A theoretical approach, compatible with what we observed, was given by Heimburg [25]. In a general overview of the formation of the ripple phase on unilamellar bilayers, he proposed that the existence of the ripple phase in water depends on the interaction energy of the bilayer with the support. He wrote the difference in total free energy ΔG as the sum of an elastic component and of another component, which results from the interaction with the environment (interaction with the solvent, with associated proteins, with surfaces). None of the terms included in the second component depend on the fusion process. They are collectively denoted ΔG_0. If they are sufficiently strong, thus if ΔG_0 is sufficiently negative, the free energy $\Delta G(T)$ can become negative close to the melting transition. In that case, the membrane will show a curvature that could lead to ripple phase formation. When DSC is performed on vesicles, it is seen that the signal has three peaks: two are separated by a temperature gap and result from pretransition and main transition respectively (width of each peak about 1 K). The third, between the two previous peaks, corresponds to the ripple phase and is greatly broadened, as shown by the fact that the curve $Cp(T)$ did not exactly come back to zero [36]. The phase transitions occur con-

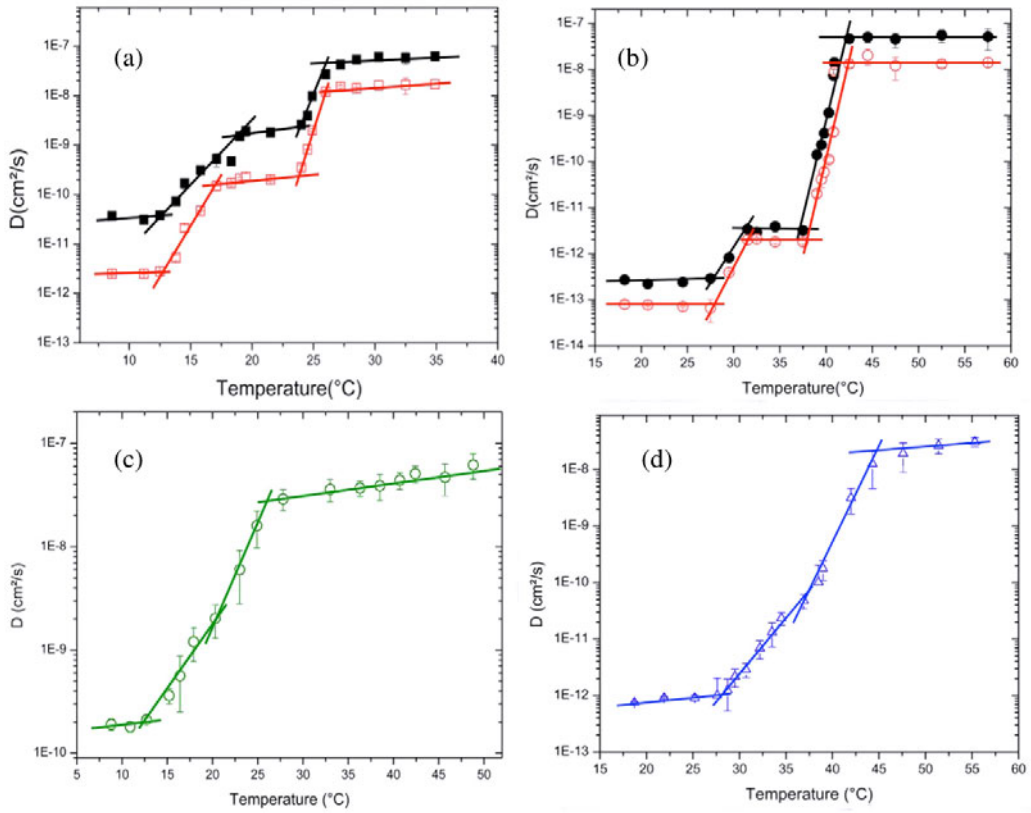

Fig. 2. Diffusion coefficient values as a function of temperature. (a) DMPC and (b) DPPC on mica. FRAPP signals are biexponential (amplitudes 50/50, relaxation time proportional to q^{-2}), which indicates that leaflets have different diffusion coefficients. The slow and the fast components are attributed to the proximal (red marks) and to the distal leaflet (black marks) respectively. (c) DMPC and (d) DPPC on glass. FRAPP signals are monoexponential, indicating that both leaflets have the same diffusion coefficient. The lines represent the fit of the curves in the different regimes.

tinuously over broad temperature ranges ($\cong 10\,\mathrm{K}$). If the interaction is strong ($\Delta G_0 < 0$), as on mica, the system will show a pretransition and a main transition linked by an intermediate ripple phase. If it is weak ($\Delta G_0 > 0$), as on glass, the pretransition will be directly followed by the main transition.

Based on our observations we conclude that:

- The existence of a plateau in the $D = f(T)$ curve denotes the existence of the ripple phase.
- A strong bilayer/support interaction can induce two consequences: leaflet decoupling, which leads to two different diffusion coefficients, and formation of the ripple phase in a given temperature range. As seen on double unilamellar-supported bilayers, a plateau can be observed without observing leaflet decoupling. This indicates that the bilayer/support interaction energy required to induce ripple formation is lower than the energy required to induce leaflet decoupling.
- If we can observe differing mobilities between distal and proximal leaflets, we can consequently hypothesize that ripples of varying thickness are induced.

The extraordinary sensitivity of lipid bilayers to experimental conditions (temperature, support material, kinetics, ionic strength, presence of mono or bivalent cations) causes widely varying behaviours, as reported in the literature. If FRAPP demonstrates that the existence of a plateau signals the existence of the ripple phase, and the ripple phase requires strong lipid-substrate interactions, it may be possible to explain or reinterpret these behaviours. Our findings may, for instance, shed new light on one aspect of the calorimetric study using AFM by Enders *et al.* [2]. Using fusion of DMPC vesicles in Hepes buffer on mica for 30 minutes to prepare the SLBs, they observed ripple structures of low amplitude. However, Enders *et al.* concluded that this was probably a double bilayer region (and not a bilayer), as proximity of the bilayer with the support may prevent large bilayer fluctuations [17,18], which in turn prevents ripple phase formation. Our results on fig. 2 show the existence of the ripple phase on DMPC bilayers on mica.

To confirm that the diffusivity plateau signals the existence of the ripple phase in unilamellar-supported bilayers, we carried out AFM experiments. Unfortunately, because of the design of the AFM device used for imaging, using the double LB deposition method for the preparation of the supported bilayer is very difficult. As in Enders *et al.* a supported lipid bilayer of DMPC was therefore prepared

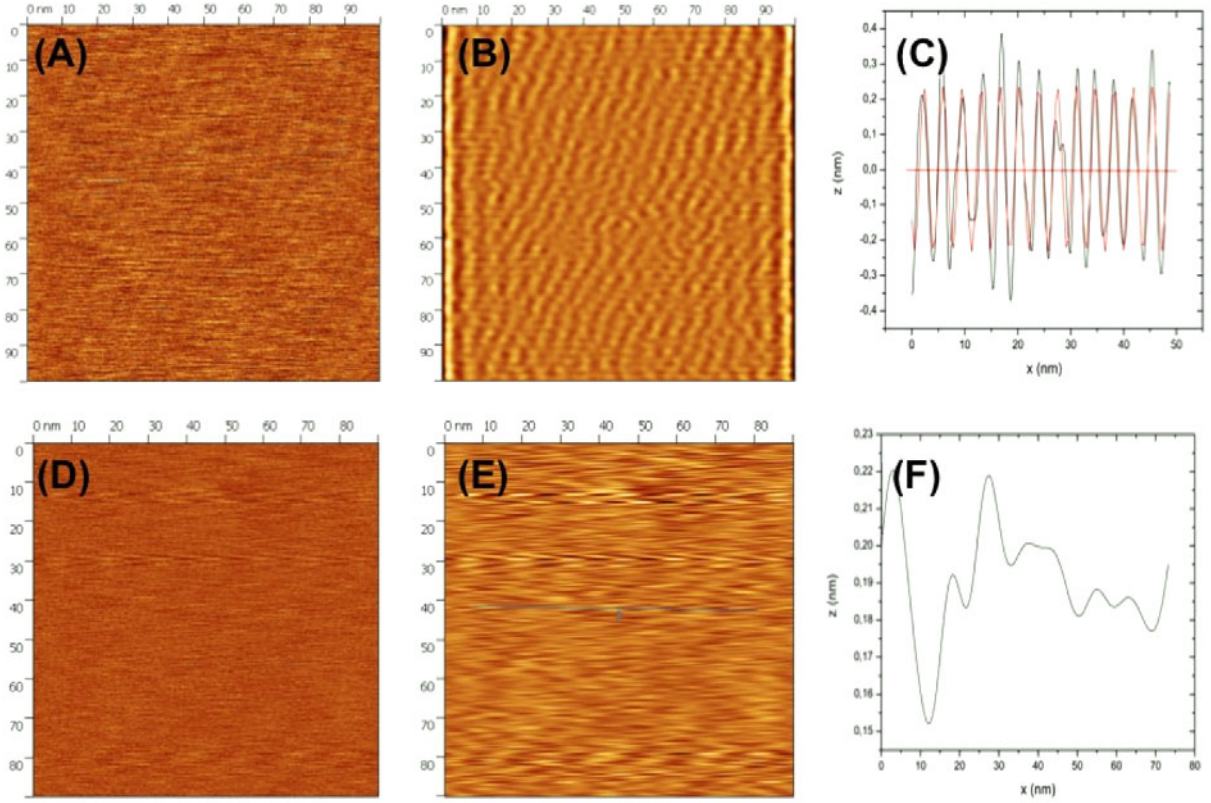

Fig. 3. AFM images of supported DMPC bilayer on mica in ultrapure water during ripple phase and after. From left to right: Flattened image, 2D FFT analysis of the image and height profile of the SLB. (A), (B) and (C) included in the temperature range at which the plateau $D = f(T)$ shows up; AFM images of the DMPC bilayer on mica. (D), (E) and (F) correspond to a temperature after the ripple phase. Image size: 100×100 nm.

by fusion of SUVs in Hepes buffer containing 150 mM and 2 mM $CaCl_2$. In the vesicle fusion method, the presence of a buffered Ca^{2+} solution ensures vesicle rupture when the surface is touched, and consequently the formation of a high quality bilayer with high coverage. All ions are considered to have been removed by extensive rinsing several times over the subsequent 12 hours, as shown by the stability of the diffusion coefficient [39] after the rinsing procedure. In other words, we consider that the resulting SLBs have the same properties and the same quality when either of the two preparation methods described in this work is used.

In fig. 3, AFM images of DMPC SLBs on mica, recorded in the temperature range for existence of the diffusivity plateau, are presented. At high magnification, the bilayer surface shows corrugated topography with height differences of $\sim$ 0.3 nm (figs. 3A, B and C) and a periodicity of 5 nm. The small amplitudes of the corrugations induce an intrinsically low contrast. The same amplitude was recorded for ripple structures with unilamellar-supported bilayers [21,39]. The low amplitude of corrugations observed in unilamellar-supported bilayers [2,21, 39] could explain why it is sometimes difficult to produce AFM images of the ripple phase and why it can be missed if not specifically sought. Other systems, with free-standing, multi or double bilayers [5,17,18,40], show amplitudes ranging from 1.5 to 11 nm. Our results exhibit qualitatively the typical structure, already well characterized by Enders *et al.* in HEPES buffer and Bayerl *et al.* in water [41], attributed to ripple phases. Given Enders' bilayer preparation conditions, we believe that their system actually corresponds to a unilamellar-supported bilayer.

To rule out any possibility of the profile height that shows the ripple phase at the plateau temperature range being an artefact, we recorded an image of the bilayer at a temperature outside the range of the ripple phase. We obtained an AFM image (figs. 3D, E and F) that does not present the ripple phase. These images confirm that the FRAPP diffusivity plateau signals the existence of the ripple phase in a unilamellar DMPC supported bilayer.

We propose this general summary:

– In systems composed of a unilamellar-supported bilayer where a strong bilayer/support interaction exists, ripples may have variable thicknesses and low amplitudes.

– In systems where the bilayer can be considered almost as a freestanding bilayer, being far away from the support (multi, double, large vesicles), ripples will have fairly constant thickness (leaflets could easily be in phase), with fluctuations showing large amplitudes.

4 Conclusion

Starting from $D = f(T)$ curves, we have shown that the existence of a diffusivity plateau is a sign of ripple phase existence. It can occur in water for a unilamellar-supported bilayer when the bilayer-support interaction is sufficiently strong, thus even in the absence of specific ions and despite the proximity of the support. This is confirmed by AFM experiments. The FRAPP technique may improve ripple phase characterization and may help identify conditions conducive to ripple phases. In particular, our work provides insights into the constant or variable thickness of the membrane in the ripple phase.

We thank Aude Lereu for helpful discussions, Jean-Paul Rieu for providing access to the Atomic Force Microscope, Marjorie Sweetko for English language editing and Aix-Marseille University for financial support to Frédéric Harb.

References

1. C. Leidy, O.G. Mouritsen, K. Jorgensen, N.H. Peters, Biophys. J. **87**, 408 (2004).
2. O. Enders, A. Ngezahayo, M. Wiechmann, F. Leisten, H.A. Kolb, Biophys. J. **87**, 2522 (2004).
3. D.C. Wack, W.W. Webb, Phys. Rev. A **40**, 2712 (1989).
4. A. Tardieu, V. Luzzati, F.C. Reman, J. Mol. Biol. **75**, 711 (1972).
5. M.J. Janiak, D.M. Small, G.G. Shipley, J. Biol. Chem. **254**, 6068 (1979).
6. S.A. Asher, P.S. Pershan, Biophys. J. **27**, 393 (1979).
7. J.A.N. Zasadzinski, M.B. Schneider, J. Phys. (Paris) **48**, 2001 (1987).
8. D. Ruppel, E. Sackmann, J. Phys. (Paris) **44**, 1025 (1983).
9. J.T. Woodward, J.A. Zasadzinski, Biophys. J. **72**, 964 (1997).
10. E.B. Sirota, G.S. Smith, C.R. Safinya, R.J. Plano, N.A. Clark, Science **242**, 1406 (1988).
11. S.J. Singer, G.L. Nicolson, Science **175**, 720 (1972).
12. K. Mortensen, W. Pfeiffer, E. Sackmann, W. Knoll, Biochim. Biophys. Acta **945**, 221 (1988).
13. S.J. Johnson, T.M. Bayerl, D.C. Mcdermott, G.W. Adam, A.R. Rennie, R.K. Thomas, E. Sackmann, Biophys. J. **59**, 289 (1991).
14. B.A. Cunningham, A.D. Brown, D.H. Wolfe, W.P. Williams, A. Brain, Phys. Rev. E **58**, 3662 (1998).
15. D. Branton, Proc. Natl. Acad. Sci. U.S.A. **55**, 1048 (1966).
16. D. Branton, J. Phys.: Conf. Ser. **351**, 12010 (2012).
17. C. Leidy, T. Kaasgaard, J.H. Crowe, O.G. Mouritsen, K. Jorgensen, Biophys. J. **83**, 2625 (2002).
18. T. Kaasgaard, C. Leidy, J.H. Crowe, O.G. Mouritsen, K. Jorgensen, Biophys. J. **85**, 350 (2003).
19. Y. Fang, J. Yang, J. Phys. Chem. **100**, 15614 (1996).
20. O. Lenz, F. Schmid, Phys. Rev. Lett. **98**, 058104 (2007).
21. J.X. Mou, J. Yang, Z.F. Shao, Biochemistry **33**, 4439 (1994).
22. H.L. Scott, W.S. Mccullough, Int. J. Mod. Phys. B **5**, 2479 (1991).
23. T.C. Lubensky, F.C. Mackintosh, Phys. Rev. Lett. **71**, 1565 (1993).
24. J.M. Carlson, S.A. Langer, J.P. Sethna, Europhys. Lett. **5**, 327 (1988).
25. H.T. Tien, A. Ottova-Leitmannova (Editors), *Planar lipid bilayers (BLMs) and their applications* (Elsevier, Amsterdam, 2003) p. 269.
26. R.E. Goldstein, S. Leibler, Phys. Rev. Lett. **61**, 2213 (1988).
27. S. Doniach, J. Chem. Phys. **70**, 4587 (1979).
28. A.H. de Vries, S. Yefimov, A.E. Mark, S.J. Marrink, Proc. Natl. Acad. Sci. U.S.A. **102**, 5392 (2005).
29. T. Heimburg, Biophys. J. **78**, 1154 (2000).
30. L.K. Tamm, H.M. Mcconnell, Biophys. J. **47**, 105 (1985).
31. B.A. Smith, H.M. Mcconnell, Proc. Natl. Acad. Sci. U.S.A. **75**, 2759 (1978).
32. H.G. Kapitza, D.A. Ruppel, H.J. Galla, E. Sackmann, Biophys. J. **45**, 577 (1984).
33. T. Charitat, E. Bellet-Amalric, G. Fragneto, F. Graner, Eur. Phys. J. B **8**, 583 (1999).
34. P. Bassereau, F. Pincet, Langmuir **13**, 7003 (1997).
35. J. Davoust, P.F. Devaux, L. Leger, Embo J. **1**, 1233 (1982).
36. T. Heimburg, Biochim. Biophys. Acta **1415**, 147 (1998).
37. C. Scomparin, S. Lecuyer, M. Ferreira, T. Charitat, B. Tinland, Eur. Phys. J. E **28**, 211 (2009).
38. F.F. Harb, B. Tinland, Langmuir **29**, 5540 (2013).
39. D.M. Czajkowsky, C. Huang, Z.F. Shao, Biochemistry **34**, 12501 (1995).
40. J.T. Woodward, J.A. Zasadzinski, Phys. Rev. E **53**, R3044 (1996).
41. T.M. Bayerl, M. Bloom, Biophys. J. **58**, 357 (1990).